Controllable color display induced by excitation-intensity-dependent competition between second and third harmonic generation in ZnO nanorods

Jun Dai,[1,2] Mao-Hui Yuan,[1] Jian-Hua Zeng,[1] Qiao-Feng Dai,[1] Sheng Lan,[1,*] Chai Xiao,[3] and Shao-Long Tie[3]

[1]Laboratory of Nanophotonic Functional Materials and Devices, School of Information and Optoelectronic Science and Engineering, South China Normal University, Guangzhou 510006, China

[2]Industrial Training Center, Guangdong Polytechnic Normal University, Guangzhou 510665, China

[3]School of Chemistry and Environment, South China Normal University, Guangzhou 510006, China

*Corresponding author: slan@scnu.edu.cn

Received 27 September 2013; revised 29 November 2013; accepted 2 December 2013; posted 4 December 2013 (Doc. ID 198426); published 6 January 2014

We investigated the second and third harmonic generation (SHG and THG) in ZnO nanorods (NRs) by using a femtosecond laser (optical parametric amplifier with tunable wavelengths) with a long excitation wavelength of 1350 nm and a low repetition rate of 1 kHz. The damage threshold for ZnO NRs in this case was sufficiently large, enabling us to observe the competition between SHG and THG. The transition from red to blue emission and the mixing of red and blue light with different ratios were successfully demonstrated by simply varying excitation intensity, implying the potential applications of ZnO NRs in all-optical display. © 2014 Optical Society of America

OCIS codes: (190.0190) Nonlinear optics; (190.2620) Harmonic generation and mixing; (260.3800) Luminescence.

http://dx.doi.org/10.1364/AO.53.000189

1. Introduction

As a semiconductor with wide bandgap and large exciton binding energy, ZnO has attracted great interest in the past decade due to its potential applications in the fabrication of optoelectronic devices [1,2]. In particular, ZnO nano-objects have been synthesized or fabricated by various chemical and physical methods, and their physical properties have received intensive and extensive studies [3,4]. Among these nano-objects, ZnO nanorods (NRs) have been the focus of many studies because of their unique mechanical, thermionic, catalytic, electrical, optical, and magnetic properties. As compared to the other properties, much effort has been devoted to the investigation of the optical properties of ZnO NRs [5–7]. In recent years, the nonlinear optical properties of ZnO, such as the second harmonic generation (SHG) [8–10], third harmonic generation (THG) [11,12], and two-photon-induced luminescence (TPL) [13–15], have attracted the interest of many researchers because of their potential applications in various fields of science and technology. The SHG in ZnO has been extensively studied, including bulk material [16], thin films [17,18], nanowires [19], nanobelts [20], and other nano-objects [10,21]. It has been shown that ZnO nanowires can be applied as miniaturized frequency converters for optical communication [22]. The second-order nonlinear susceptibility for bulk ZnO was measured to be $\chi_{33}^{(2)} = 14.31 \pm 0.4$ pm/V [16]. In addition, it was found that the second-order susceptibility of ZnO films increased with decreasing thickness [18]. In most

1559-128X/14/020189-06$15.00/0

studies, however, the nonlinear optical signals of ZnO NRs are generated using a femtosecond (fs) laser at wavelengths ranging from 700 to 800 nm. As a result, only SHG and TPL are observed in the nonlinear optical response of ZnO NRs. For example, enhanced SHG was observed in ZnO NRs when the excitation wavelength was tuned to the exciton ground state [23]. Very recently, we demonstrated the competition between SHG and TPL observed in gold nanoparticles (NPs) [24] and in single, double, and multiple ZnO NRs [25], implying that their nonlinear optical properties depend strongly on the absorption and scattering properties of gold NPs or ZnO NRs. In addition, it was revealed that the strong TPL related to the generation of real carriers led to a significant temperature rise in gold NPs and ZnO NRs.

As compared to SHG and TPL, the investigation of THG in ZnO NRs is very rare possibly because of several reasons. First, the third-order nonlinear susceptibility of ZnO is about 10 orders of magnitude smaller than the second-order one [26,27], and its intensity is quite weak when a fs oscillator with a high repetition rate is employed. Second, the THG of ZnO NRs appears in the ultraviolet region where the detection is not easy when an excitation wavelength of ~800 nm is used. Finally, the temperature rise accompanied with the TPL leads to the damage of ZnO NRs at high excitation intensities. Recently, the spatial distributions of SHG and THG in single ZnO nanowires were investigated by using scanning near-field microscopy [19]. It was also proposed that under certain experimental conditions, THG with intensity comparable to that of SHG can be observed in ZnO thin films. However, the demonstration of a dynamical competition between SHG and THG is still lacking.

For materials with centrosymmetry such as silicon, SHG is not allowed for bulk material but is possible at interfaces where the symmetry is broken. In this case, the intensity of THG may be stronger than that of SHG at low excitation intensities [28]. For materials with large second-order susceptibilities such as ZnO, it is easy to observe SHG whose intensity is generally stronger than THG. In rare cases, the THG can be much stronger than SHG even at low excitation intensities [11].

Basically, the intensity of SHG scales quadratically with the intensity of the excitation light while that of THG exhibits a cubic dependence on the excitation intensity. Therefore, it is expected that there exists excitation-intensity-dependent competition between these two nonlinear optical processes. While SHG is dominant at low excitation intensities, the nonlinear response will eventually be governed by THG at high excitation intensities. In order to observe such a competition, the damage threshold for ZnO NRs needs to be large enough so that the intensity of THG can exceed that of SHG. However, the excitation intensity at which the intensity of THG becomes equal to that of SHG is generally quite large. The heat generated by multiphoton absorption processes will lead to damage of ZnO before such an excitation intensity is reached. Therefore, it is necessary to suppress the multiphoton absorption processes in order to observe the competition between SHG and THG. In addition, single-photon absorption of the third harmonic must be avoided. For this reason, an excitation wavelength much longer than 800 nm is preferred.

In this article, we report on the simultaneous presence of SHG and THG in ZnO NRs by using a fs laser at 1350 nm. The competition between them was successfully demonstrated by either moving the focusing lens or simply changing the power of the fs laser. It was clearly reflected in the transition of the emission light color from red to blue, implying that the color of the emission light can be easily controlled by focusing (or defocusing) the laser beam or adjusting the laser power, making ZnO NRs promising candidates for all-optical display.

2. Experimental Section

The ZnO NRs used in our study were synthesized by using the method reported previously [25,29]. The detailed synthesis process and scanning electron microscope images of ZnO NRs can be found in our previous publications [29,30]. The average diameter and length of ZnO NRs were measured to be ~250 nm and ~2 μm. They were compressed as a thin film with a thickness of ~100 μm for optical measurements.

For the characterization of the SHG and THG in ZnO NRs, we employed an optical parametric amplifier (OPerA Solo, Coherent) with a repetition rate of 1 kHz. The excitation wavelength (λ_{ex}) was chosen to be 1350 nm so that SHG and THG gave rise to typical red and blue emissions, respectively. In addition, single-photon absorption of the third harmonic was avoided and only four-photon absorption (4PA) with a very small absorption coefficient was allowed because the energy of three photons was still smaller than the energy of the exciton ground state. In this case, the possibility for real carrier generation was quite small, leading to a large damage threshold for ZnO NRs. As schematically shown in Fig. 1, the fs laser light was focused on the ZnO sample by using a lens with a focusing length of ~150 mm at an angle of 45°, while the generated nonlinear optical signals were collected by using another lens and directed to a spectrometer for analysis. In the experiments described in the following, the sample was placed 2 and 1 cm away from the focus and the diameters of the excitation spot were estimated to be ~187 and 125 μm, respectively. A lock-in amplifier was used to enhance the signal-to-noise ratio. As discussed above, the competition between SHG and THG can be observed by varying the excitation intensity (I_{ex}). In experiments, we changed the excitation intensity of the pump light by either moving the focusing lens or adjusting the pump power, as depicted in Fig. 1. The excitation intensities given in this

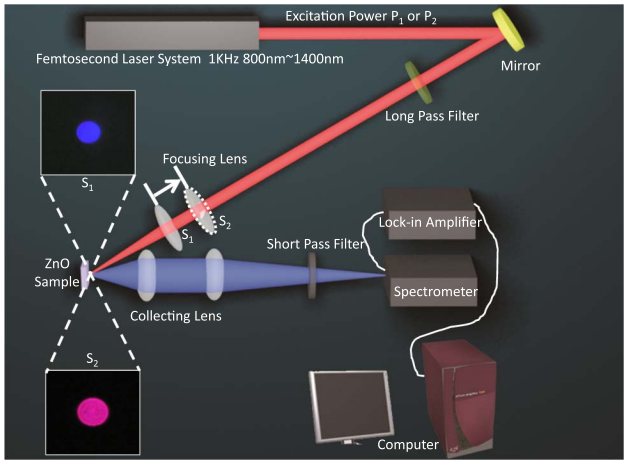

Fig. 1. Schematic showing the experimental setup used to observe the transition from red to blue emission resulting from the competition between SHG and THG. The excitation intensity was changed by either moving the focusing lens or adjusting the power of the fs laser. The images of the excitation spot recorded by a camera at two different positions of the focusing lens are presented.

paper are obtained by dividing the peak power of the fs laser pulses with the excitation spot size.

3. Results and Discussion

We first examined the excitation-wavelength-dependent SHG and THG in ZnO NRs, as shown in Fig. 2. The sample was placed 2 cm away from the focus, and the excitation intensity was fixed at 0.12 TW/cm^2. In Fig. 2, the SHG intensities for three excitation wavelengths were normalized in order to compare the relative intensities of the THG. It can be seen that the THG intensity decreased with decreasing excitation wavelength. In particular, a significant reduction in the THG intensity was observed when the excitation wavelength was tuned to 1150 nm. In this case, the energy of the third harmonic became larger than that of the exciton ground state and the THG was reduced by reabsorption. In addition, three-photon-induced luminescence through three-photon absorption (3PA) also became

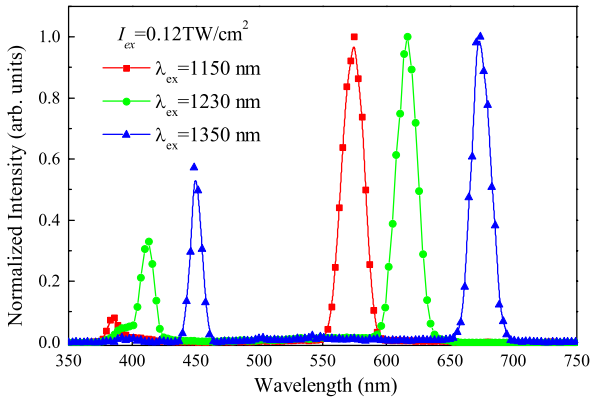

Fig. 2. Nonlinear response spectra obtained at different excitation wavelengths of 1150, 1230, and 1350 nm. The ZnO sample was placed 2 cm away from the focus, and the excitation intensity was fixed at 0.12 TW/cm^2.

possible, although it was not pronounced. Previously, the typical excitation wavelengths used to investigate the SHG and THG of ZnO were 800 and 1064 nm [12,18,26,31]. Thus, the intensity of THG was much weaker as compared to that of SHG, making it difficult to observe the competition between these two nonlinear optical processes. Therefore, we think that a long excitation wavelength at which 3PA and reabsorption of the third harmonic are avoided is preferred in order to observe the competition between SHG and THG.

In Fig. 2, it can be seen that the intensity of SHG is larger than that of THG at an excitation intensity of 0.12 TW/cm^2 because of the larger second-order susceptibility. In order to realize the reverse situation in which THG is stronger than SHG, we need to increase the excitation intensity. From the viewpoint of experiment, a simple way to do that is to move the focusing lens or to increase the power of the fs laser. In Fig. 3, we present the evolution of the nonlinear response spectrum when the focusing lens was moved from the initial position, which was 2 cm away from the focus, toward the focus. During the movement, we recorded the nonlinear response spectrum with

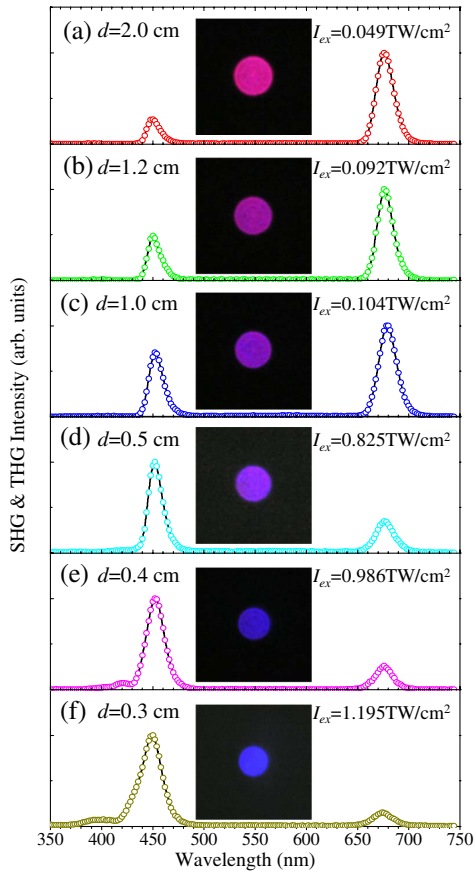

Fig. 3. Evolution of the nonlinear response spectrum of ZnO NRs when the focusing lens was moved from the initial position (2 cm away from the focus) toward the focus. The corresponding images of the excitation spot recorded by using a camera are presented as insets. In each case, the estimated excitation intensity and the distance between the sample and the focus (d) are provided.

the spectrometer and took the image of the excitation spot with a camera. The results at several positions are shown in Fig. 3. Initially, we observed a red spot with a circular shape and a large diameter. Then, it was changed to a violet spot with a middle size. Finally, a blue spot with a small diameter was observed. This transition from a red spot to a blue one is in good agreement with the evolution of the nonlinear response spectrum presented in Fig. 3. It should be emphasized that the emission spot size does not reflect the real excitation spot size because it appears to be larger under higher excitation intensities.

Another way to increase the intensity of the THG is to simply increase the power of the fs laser. In this case, the evolution of the nonlinear response spectrum with increasing excitation intensity is shown in Fig. 4(a). At a low excitation intensity of 0.10 TW/cm^2, SHG was stronger than THG. As the excitation intensity was increased to 0.20 TW/cm^2, the difference between SHG and THG became smaller, although the former was still stronger than the latter. At a high excitation intensity of 0.40 TW/cm^2, THG exceeded SHG and dominated the nonlinear response spectrum. The excitation intensity dependences of SHG and THG are plotted in Fig. 4(b). The slopes derived for the excitation-intensity-dependent SHG and THG are 1.80 and 2.83, which are in good agreement with the second-order and third-order nonlinear optical processes. It can be seen clearly that the intensity of THG becomes equal to that of SHG at an excitation intensity of ~0.25 TW/cm^2. After that, THG is stronger than SHG. However, a gradual saturation is observed for both SHG and THG at high excitation intensities, which is reflected in the reduction of their slopes.

It has been shown that the intensity of THG can exceed that of SHG by simply increasing the excitation intensity. In this case, it is assumed that 4PA can be neglected because of the small absorption coefficient. However, this assumption is no longer valid at high excitation intensities because 4PA is expected to increase more rapidly than THG. In order to see the competition between these three nonlinear processes, we first moved the focusing lens so that the ZnO sample was located 1 cm from the focus and then increased the excitation power. In this case, the diameter of the excitation spot was reduced to ~125 μm. The evolution of the nonlinear response spectrum with increasing excitation intensity is shown in Fig. 5(a). When the excitation density is increased to 0.513 TW/cm^2, a broad emission peaking at 390 nm begins to appear in the spectrum. Its intensity increased when the excitation intensity was

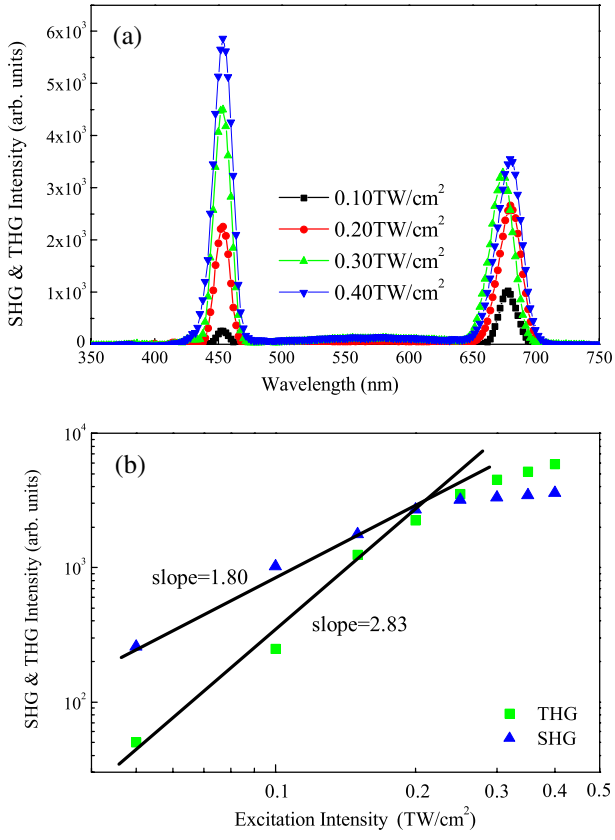

Fig. 4. (a) Evolution of the nonlinear response spectrum of ZnO NRs with increasing excitation intensity. (b) Excitation-intensity-dependent SHG and THG of ZnO NRs. Circles and squares are experimental data, and the solid lines are the fits to these data.

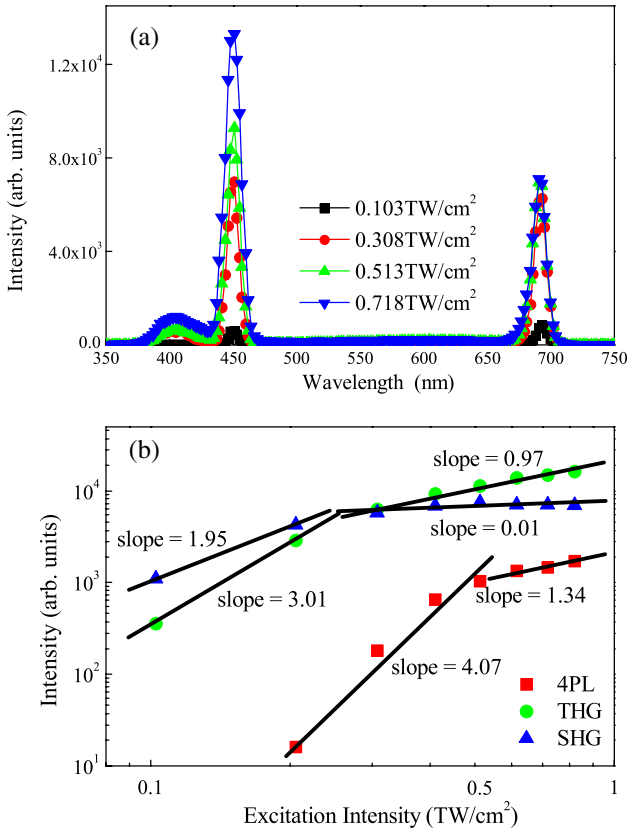

Fig. 5. (a) Evolution of the nonlinear response spectrum of ZnO NRs with increasing excitation intensity. (b) Excitation-intensity-dependent SHG, THG, and 4PL of ZnO NRs. Squares, circles, and triangles are experimental data, and the solid lines are the fits to these data.

further increased to 0.718 TW/cm^2. This emission is attributed to the exciton emission resulting from the 4PA in ZnO NRs. Thus, it belongs to a four-photon luminescence (4PL).

In order to gain deep insight into the competition between SHG, THG, and 4PL with increasing excitation intensity, the excitation intensity dependences of these nonlinear optical signals are presented in Fig. 5(b). In each case, the excitation-intensity-dependent signal can be classified into two regimes in which the slopes were found to be different. For SHG, a significant reduction of the slope from 1.95 to 0.01 was observed, indicating the saturation of the SHG at high excitation intensities due to energy redistribution or energy transfer. A similar phenomenon was observed for THG, and its slope was found to decrease from 3.01 to 0.97 in the high excitation intensity regime. The transition from a large slope to a small one occurred at the same excitation intensity for SHG and THG. For 4PL, a decrease of the slope from 4.07 to 1.34 was found at a higher excitation intensity of 0.50 TW/cm^2 where the damage of ZnO NRs might occur due to the significant temperature rise caused by the 4PA. When we compare the excitation-intensity-dependent SHG and THG shown in Fig. 4(b) with that shown in Fig. 5(b), it is found that the intensities of SHG and THG become equal at nearly the same excitation intensity of 0.25 TW/cm^2 in both cases. However, a rapid saturation of SHG and THG as well as a rapid increase in 4PL is observed in the latter case because of the smaller excitation spot. It implies that the competition between different nonlinear optical processes occurring in nanostructures depends not only on the excitation intensity but also on the excitation spot size. It is thought that the excitation spot size may influence the excitation volume and temperature rise in nanostructures. Based on our experimental observations, it is suggested that nonlinear optical processes with higher orders, such as 4PL in our case, will be facilitated by employing a small excitation spot size. Of course, more experiments are needed to clarify this issue.

For practical applications, the optical damage of ZnO NRs under high excitation intensities needs to be considered. The damage threshold for ZnO was reported to be ~5 TW/cm^2 at an excitation wavelength of 800 nm [32]. It is expected to be larger at longer excitation wavelengths because of the suppression of multiphoton absorption. The excitation intensities used in our experiments were carefully controlled to be much lower than the damage threshold. In order to observe the competition between SHG and THG without damaging the sample, the excitation wavelength was intentionally chosen at 1350 nm so that the multiphoton absorption was greatly suppressed. The reduction in the slopes of the excitation-intensity-dependent SHG and THG (or the saturation of SHG and THG) observed at high excitation intensities was caused mainly by the rapid increase in the multiphoton-absorption-induced luminescence, not the damage of the sample. It was confirmed by the fact that the excitation intensity dependences of SHG and THG can be reproduced.

Another issue that needs to be taken into account is phase matching, which is quite important for realizing efficient SHG and THG in bulk materials. For micro- and nanostructures, however, it has been demonstrated that the efficiency of SHG and THG can be greatly enhanced at the surfaces, especially for closely packed micro- and nanostructures [33–35]. As a result, the excitation intensity for efficient SHG and THG is reduced significantly. On the other hand, one can consider a film composed of micro- and nanostructures whose sizes are comparable to or smaller than the wavelength of light as a composite with an effective refractive index. The phase matching in SHG and THG can still be satisfied by deliberately designing the parameters of the composite.

4. Conclusion

In summary, we have demonstrated the competition between SHG and THG in ZnO NRs by employing a fs laser with a long excitation wavelength of 1350 nm and a low repetition rate of 1 kHz. A transition from red to blue emission resulting from the competition between SHG and THG was successfully demonstrated by simply increasing excitation intensity. This property of ZnO NRs may find potential applications in the fields of all-optical display and intensity measurements.

The authors acknowledge financial support from the National Natural Science Foundation of China (Grant Nos. 51171066 and 11374109), the Ministry of Education of China (Grant No. 20114407110002), and the project for high-level professionals in the universities of Guangdong province, China. Q.-F. Dai thanks financial support from the Guangzhou Pearl River New-star Plan of Science and Technology (Grant No. 2011J2200080).

References

1. D. M. Bagnall, Y. F. Chen, Z. Zhu, T. Yao, S. Koyama, M. Y. Shen, and T. Goto, "Optically pumped lasing of ZnO at room temperature," Appl. Phys. Lett. **70**, 2230–2232 (1997).
2. A. B. Djurišić and Y. H. Leung, "Optical properties of ZnO nanostructures," Small **2**, 944–961 (2006).
3. O. Mondal and M. Pal, "Strong and unusual violet-blue emission in ring shaped ZnO nanocrystals," J. Mater. Chem. **21**, 18354–18358 (2011).
4. M. H. Huang, S. Mao, H. Feick, H. Yan, Y. Wu, H. Kind, E. Weber, R. Russo, and P. Yang, "Room-temperature ultraviolet nanowire nanolasers," Science **292**, 1897–1899 (2001).
5. B. Jin and D. Wang, "Strong violet emission from zinc oxide dumbbell-like microrods and nanowires," J. Lumin. **132**, 1879–1884 (2012).
6. J. L. Zeng, X. W. Zhang, J. Z. Yie Tan, J. C. Bian, Z. Li, Z.-D. Chen, R.-Q. Peng, H.-Y. He, J. Wang, and F. Yang, "Full-color photoluminescence of ZnO nanorod arrays based on annealing processes," J. Lumin. **135**, 201–205 (2013).
7. H. B. Zeng, G. T. Duan, Y. Li, S. K. Yang, X. X. Xu, and W. P. Cai, "Blue luminescence of ZnO nanoparticles based on non-equilibrium processes: defect origins and emission controls," Adv. Funct. Mater. **20**, 561–572 (2010).

8. S. W. Liu, H. J. Zhou, A. Ricca, R. Tian, and M. Xiao, "Far-field second-harmonic fingerprint of twinning in single ZnO rods," Phys. Rev. B **77**, 113311 (2008).
9. S. W. Chan, R. Barille, J. M. Nunzi, K. H. Tam, Y. H. Leung, W. K. Chan, and A. B. Djurišić, "Second harmonic generation in zinc oxide nanorods," Appl. Phys. B **84**, 351–355 (2006).
10. S. K. Das, M. Bock, C. O'Neill, R. Grunwald, K. M. Lee, L. Hwang Woon, S. Lee, and F. Rotermund, "Efficient second harmonic generation in ZnO nanorod arrays with broadband ultrashort pulses," Appl. Phys. Lett. **93**, 181112 (2008).
11. J. Jang, S. Park, N. Frazer, J. Ketterson, S. Lee, B. Roy, and J. Cho, "Strong P-band emission and third harmonic generation from ZnO nanorods," Solid State Commun. **152**, 1241–1243 (2012).
12. H. Lee, K. Lee, S. Lee, K. Koh, J.-Y. Park, K. Kim, and F. Rotermund, "Ultrafast third-order optical nonlinearities of vertically aligned ZnO nanorods," Chem. Phys. Lett. **447**, 86–90 (2007).
13. S. K. Das, M. Biswas, D. Byrne, M. Bock, E. McGlynn, M. Breusing, and R. Grunwald, "Multiphoton-absorption induced ultraviolet luminescence of ZnO nanorods using low-energy femtosecond pulses," J. Appl. Phys. **108**, 043107 (2010).
14. C. F. Zhang, Z. Dong, K. Liu, Y. Yan, S. Qian, and H. Deng, "Multiphoton absorption pumped ultraviolet stimulated emission from ZnO microtubes," Appl. Phys. Lett. **91**, 142109 (2007).
15. C. F. Zhang, F. Zhang, S. Qian, N. Kumar, J.-I. Hahm, and J. Xu, "Multiphoton absorption induced amplified spontaneous emission from biocatalyst-synthesized ZnO nanorods," Appl. Phys. Lett. **92**, 233116 (2008).
16. G. Wang, G. K. L. Wong, and J. B. Ketterson, "Redetermination of second-order susceptibility of zinc oxide single crystals," Appl. Opt. **40**, 5436–5438 (2001).
17. M. Larciprete, D. Haertle, A. Belardini, M. Bertolotti, F. Sarto, and P. Günter, "Characterization of second and third order optical nonlinearities of ZnO sputtered films," Appl. Phys. B **82**, 431–437 (2006).
18. G. Wang, G. Kiehne, G. Wong, J. Ketterson, X. Liu, and R. Chang, "Large second harmonic response in ZnO thin films," Appl. Phys. Lett. **80**, 401–403 (2002).
19. J. C. Johnson, H. Yan, R. D. Schaller, P. B. Petersen, P. Yang, and R. J. Saykally, "Near-field imaging of nonlinear optical mixing in single zinc oxide nanowires," Nano Lett. **2**, 279–283 (2002).
20. Z. K. Zhou, Z. H. Hao, Z. W. Mei, X. G. Wen, and S. H. Yang, "Nonlinear photoluminescence from ZnO nanobelts," Chin. Phys. Lett. **26**, 024201 (2009).
21. U. Neumann, R. Grunwald, U. Griebner, G. Steinmeyer, and W. Seeber, "Second-harmonic efficiency of ZnO nanolayers," Appl. Phys. Lett. **84**, 170–172 (2004).
22. E. V. Dorote, ed., *Trends in Nanotechnology Research* (Nova Science, 2004).
23. R. Prasanth, L. K. van Vugt, D. A. M. Vanmaekelbergh, and H. C. Gerritsen, "Resonance enhancement of optical second harmonic generation in a ZnO nanowire," Appl. Phys. Lett. **88**, 181501 (2006).
24. H. Deng, G. Li, Q. Dai, M. Ouyang, S. Lan, V. A. Trofimov, and T. M. Lysak, "Size dependent competition between second harmonic generation and two-photon luminescence observed in gold nanoparticles," Nanotechnology **24**, 075201 (2013).
25. J. Dai, J. H. Zeng, S. Lan, X. Wan, and S. L. Tie, "Competition between second harmonic generation and two-photon-induced luminescence in single, double and multiple ZnO nanorods," Opt. Express **21**, 10025–10038 (2013).
26. B. Kulyk, Z. Essaidi, J. Luc, Z. Sofiani, G. Boudebs, B. Sahraoui, V. Kapustianyk, and B. Turko, "Second and third order nonlinear optical properties of microrod ZnO films deposited on sapphire substrates by thermal oxidation of metallic zinc," J. Appl. Phys. **102**, 113113 (2007).
27. V. Narayanan and R. Thareja, "Harmonic generation in ZnO nanocrystalline laser deposited thin films," Opt. Commun. **260**, 170–174 (2006).
28. T. Y. Tsang, "Optical third-harmonic generation at interfaces," Phys. Rev. A **52**, 4116–4125 (1995).
29. J. Dai, Z. Fu, S. Lan, X. Wan, S. Tie, V. A. Trofimov, and T. M. Lysak, "Modified threshold of two-photon-pumped random lasing of ZnO nanorods by femtosecond laser ablation," J. Appl. Phys. **112**, 063101 (2012).
30. Z. C. Fu, J. Dai, T. Li, H. Y. Liu, Q. F. Dai, L. J. Wu, S. Lan, S. L. Tie, X. Wan, A. V. Gopal, V. A. Trofimov, and T. M. Lysak, "Femtosecond laser ablation of ZnO nanorods for two-photon-pumped random lasing and optical data storage," Appl. Phys. B **108**, 61–66 (2012).
31. C. Liu, B. Zhang, N. Binh, and Y. Segawa, "Third-harmonic generation from ZnO films deposited by MOCVD," Appl. Phys. B **79**, 83–86 (2004).
32. O. Mücke, T. Tritschler, M. Wegener, U. Morgner, and F. Kärtner, "Determining the carrier-envelope offset frequency of 5-fs pulses with extreme nonlinear optics in ZnO," Opt. Lett. **27**, 2127–2129 (2002).
33. J. Zhang, L. Wang, S. Krishna, M. Sheik-Bahae, and S. Brueck, "Saturation of the second harmonic generation from GaAs-filled metallic hole arrays by nonlinear absorption," Phys. Rev. B **83**, 165438 (2011).
34. M. Nayfeh, O. Akcakir, G. Belomoin, N. Barry, J. Therrien, and E. Gratton, "Second harmonic generation in microcrystallite films of ultrasmall Si nanoparticles," Appl. Phys. Lett. **77**, 4086–4088 (2000).
35. C. Q. Li, C. Y. Zhang, Z. S. Huang, X. F. Li, Q. F. Dai, S. Lan, and S. Tie, "Assembling of silicon nanoflowers with significantly enhanced second harmonic generation using silicon nanospheres fabricated by femtosecond laser ablation," J. Phys. Chem. C **117**, 24625–24631 (2013).